CHAPTER : 2 π - delocalized bi-bridged binuclear complexes.

2.1 Introduction

2.2 Experimental

2.3 Results and Discussion

2.4 References

2.1 Introduction

In recent years the study of binuclear copper (II) complexes has been a subject of considerable interest. This is mainly because of the special structural, magnetic and ESR properties associated with them [1-5]. Some of these compounds can also provide good models for bi/multinuclear active sites in metalloenzymes [6-11]. The catalytic activity of these binuclear centres can be probably attributed to their redox characteristics which are expected to be affected by the magnetic exchange and existence of a suitable path to mediate the spin / electronic exchange. Unlike complexes with single atom bridges where direct super exchange can take place, polyatomic bridging units function in a more complex manner. Studies of complexes with different geometries around the metal ion and with binucleating ligands possessing σ and π – orbitals have clearly indicated that the spin – spin interaction is dependent on the availability of bridge molecular orbitals with the correct symmetry and energy to propagate interaction between the metal orbitals in which the unpaired electron resides [12-14].

The aromatic bridging groups or the groups with highly conjugated π – systems have more number of closely spaced molecular orbitals to match with the paramagnetic orbitals of the metal ions. Hence, these in general can be expected to be better mediators of magnetic exchange. Nitrogen heterocycles like pyrazolate, pyrimidine, pyrazine and various triazine as well as a number of oxalate type bridging ligands are proved to be efficient mediators of spin interaction for this reason [15-19]. Earlier in our laboratory Copper (II) complexes of binucleating ligands with two bidentate sites separated by one aromatic ring have been studied and the possibility of isomeric ligands having different ability to mediate magnetic exchange was indicated [20].

In present work an attempt is made to synthesize new homo binuclear complexes of copper(II) of the type $[Cu_2L_2]$, H_2L= bis(2'-hydroxybenzylidene-4-iminophenyl)methane, bis(2'-hydroxybenzylidene-4-iminophenyl)ether, bis(2'-hydroxybenzylidene-4-iminophenyl)sulphone, bis(2'-hydroxybenzylidene-3-

iminophenylsulphone and their derivatives with substitution on hydroxy phenyl part of the ligands. The complexes have been synthesised and characterized by analysis and by various spectral techniques. The resulting complexes were characterised by elemental analysis, UV-VIS, IR, ESR and Mass spectral techniques. The variable temperature magnetic measurments have been carried out to study the presence of long range spin exchange interaction. Molecular modelling by force field calculation has been used to work out the geometrical parameters in various complexes. The magnetic properties have been analysed on the basis of the structural parameters related to the ligands and substituents present on them.

2.2 Experimental

2.2.1 Chemicals:

2-Hydroxybenzaldehyde (Aldrich), 2-hydroxynaphthaldehyde (Fluka), 4,4'-diaminodiphenylmethane, 4,4'-diaminodiphenylether, 4,4'-diaminodiphenylsulphone, 3,3'-diaminodiphenylsulphone, glacial acetic acid and cupric acetate monohydrate were purchased from Merck. All these reagents were AR grade and were used as received. o-Vanillin (LR) was obtained from local manufacturers.

5-bromo-2-hydroxybenzaldehyde (Brsal) was prepared by the method reported earlier [21].

All solvents were distilled twice before use.

2.2.2 Physical measurements:

Carbon, Hydrogen and Nitrogen analysis were carried out on a Perkin Elamer Model-2400 CHN/S analyser.

The thermogravimetric analysis of the complexes was carried out by using thermal analyser, Mettler Toledo SW 7.01 instrument in nitrogen atmosphere with a heating rate of 5 °C/min.

^{1}H NMR and ^{13}C of the ligand was recorded on Brucker DPX 200 MHz instrument.

IR spectra were recorded in the forms of KBr pellets on Perkin Elamer FT-IR, spectrum RX1 spectrometer.

The electronic spectra of the complexes in UV-VIS region were recorded in methanolic solutions using Shimadzu UV-240 recording spectrophotometer. The diffuse reflectance spectra were recorded on the same instrument, equipped with spherical reflectance assembly using $BaSO_4$ as a reference material.

The ESR spectra of the complex $[Cu_2(BrsalDPM)_2]$ at LNT and RT were recorded on a Varian E-15 spectrometer.

The FAB mass spectrum of the complex $[Cu_2(BrsalDPM)_2]$ in m-nitrobenzyl alcohol matrix was recorded on a JEOLSX 102/DA – 6000 mass spectrometer / Data system. Argon (6 KV, 10 mA) was used as a FAB gas. The spectra were recorded at room temperature with an accelerating voltage of 10 KV.

Magnetic Susceptibility measurements were carried out on solid samples in the 90–300 K temperature range with an indigenous Faraday set up as illustrated in **Fig. 2.1.**

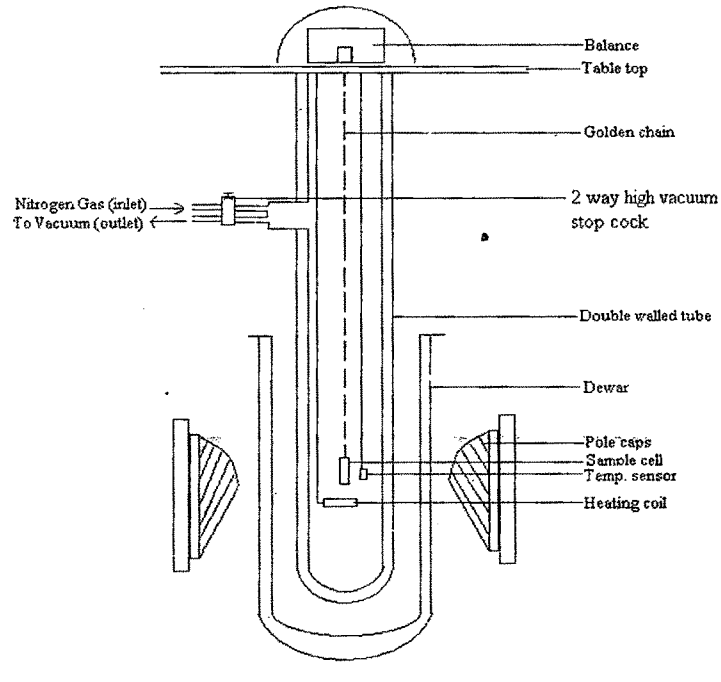

Fig. 2.1 Schematic diagram of the Faraday set up.

The set up has an electromagnet, POLYTRONIC electromagnet Model: HEM - 200 with highest field strength of 1 Tesla and Faraday pole caps with a 30 mm pole gap. A METTLER ultramicro balance, Model UMX - 5 Comparator with hang down facility is used for weighing procedure. The balance has 5 mg capacity with ±0.1 μg accuracy and 0.1 μg, readability. The sample cell is hanged down the balance in a vacuum enclosure, surrounded by a liq. N_2 bath such that the sample is positioned between the pole caps. A miniature non-magnetic heater and temperature sensor (Pt resistor) are positioned along side the sample cell. The temperature inside the sample enclosure was maintained with the help of OMEGA CYC 3200, Auto-tunning Temperature Controller having an accuracy of 0.01°.

The sample in the cell was suspended from the balance with a gold chain and positioned between the pole caps within the area of constant field gradient, H.dH/dx. The vacuum enclosure was purged several times with pure N_2 and then evacuated. The weight of the sample was noted. Sample temperature was lowered by filling the outer Dewer by liq. N_2 and allowing to stand until the temperature became constant. Then on the temperature of the sample was gradually increased with the help of temperature controller and at each temperature the weight of the sample with and without magnetic field was noted. All measurements were done at a field strength of 0.8 Tesla. The sample cell was calibrated with $Hg[Co(SCN)_4]$ as calibrant. The magnetic susceptibility was calculated using the following formula.

$$\chi_g = HdH.dw/dx.$$

Where, the terms have their usual meaning.

Magnetic susceptibility of the binuclear copper (II) complex per copper atom was calculated using the following equation,

$$\chi_A = \chi_g . \text{mol.wt.} / 2$$

Diamagnetic corrections were incorporated using Pascal's constants. The effective magnetic moments were calculated by the formula-

$$\mu_{eff} = (3k/N_A\mu_B)^{1/2}(\chi_A T)^{1/2}$$

A least-squares calculations were performed by fitting the experimentally observed values of magnetic susceptibility at various temperature to Bleaney-Bower's equation [22,23]

$$\chi = g^2 N\mu_B{}^2/3kT\,[1+1/3\exp(-2J/kT] + N\alpha$$

The difference $|\chi^2_{calc} - \chi^2_{obsd}|$ was minimised to get the values of coupling constant J, which is a measure of the magnetic exchange between the copper (II) ions and $N\alpha$ is temperature independent paramagnetism i.e. 60 emu/mole, per copper ion.

2.2.3 Synthesis of binucleating Schiff base ligands:

Preparation of H_2salDPM (H_2L^{1a}):

4,4'-Diaminodiphenylmethane (0.99 g, 5mmols) was dissolved in 60 ml of methanol. 2-Hydroxybenzaldehyde (1.22 g, 10 mmols) was added to the solution, followed by 2 ml of glacial acetic acid to facilitate the reaction. The reaction mixture was allowed to reflux for two hours at the end of which a bright yellow coloured compound separated. The solid obtained was filtered and washed with CH_3OH (15 ml) and dried. The compound was recrystallised from hot $CHCl_3$. Yield:72 %, mp. 225 °C.

Ligands H_2salDPE (H_2L^{1b}), H_2sal4-DPS (H_2L^{1d}), H_2naphDPM (H_2L^{2a}), H_2naph4-DPS (H_2L^{2d}), H_2vanDPM (H_2L^{3a}), H_2van4-DPS (H_2L^{3d}), H_2BrsalDPM (H_2L^{4a}), and H_2Brsal4-DPS (H_2L^{4d}) were prepared by similar methods as H_2L^{1a}, using equivalent quantities of respective aldehydes and amines as shown in **scheme 2.1.** The yields, mp and the result of elemental analysis are summarized in **Table 2.1.**

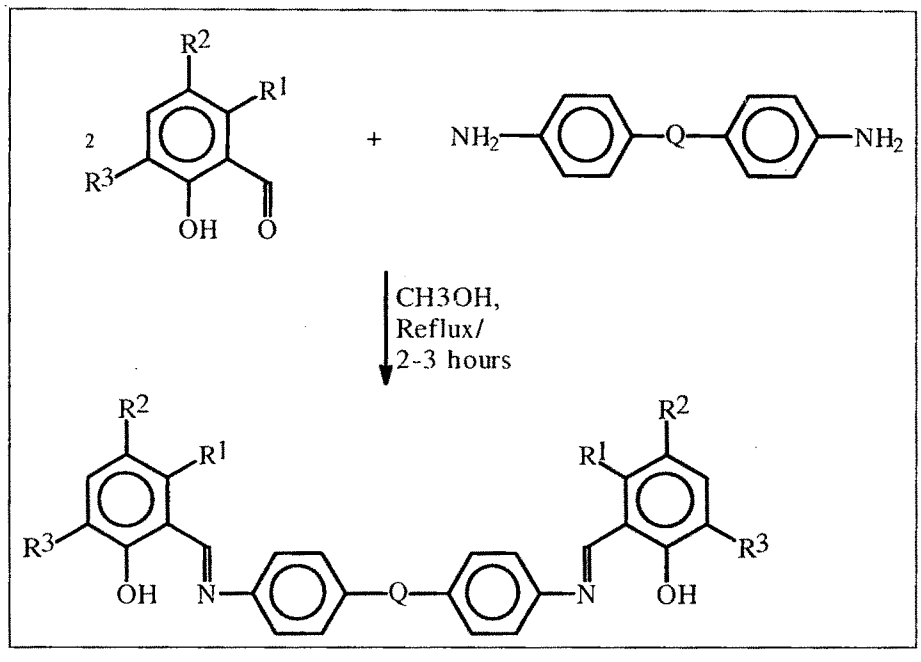

H_2L^{1a} to H_2L^{1d}
H_2L^{2a} & H_2L^{2d}
H_2L^{3a} & H_2L^{3d}
H_2L^{4a} to H_2L^{4d}

(Scheme- 2.1)

H_2L^{1a} = bis{4-(2-hydroxybenzyl)iminophenyl}methane

H_2L^{1b} = bis{4-(2-hydroxybenzyl)iminophenyl}ether

H_2L^{1d} = bis{4-(2-hydroxybenzyl)iminophenyl}sulphone

H_2L^{2a} = bis{4-(2-hydroxynaphthyl)iminophenyl}methane

H_2L^{2d} = bis{4-(2-hydroxynaphthyl)iminophenyl}sulphone

H_2L^{3a} = bis{4-(2-hydroxy-3-methoxybenzyl)iminophenyl}methane

H_2L^{3d} = bis{4-(2-hydroxy-3-methoxybenzyl)iminophenyl}sulphone

H_2L^{4a} = bis{4-(5-bromo-2-hydroxybenzyl)iminophenyl}methane

H_2L^{1a} = bis{4-(5-bromo-2-hydroxybenzyl)iminophenyl}methane

Table 2.1: Preparative yields, mp and analytical data of the binucleating Schiff bases.

	Ligands	Yields (%)	Mp. (°C)	Elemental analysis Found (Calc)* %		
				C	H	N
H_2L^{1a}	[H_2salDPM]	72	225	79.81	5.31	7.02
	$C_{27}H_{22}N_2O_2$			(79.80)	(5.42)	(7.89)
H_2L^{1b}	[H_2salDPE]	64	192	77.79	4.66	7.38
	$C_{26}H_{20}N_2O_3$			(76.46)	(4.90)	(6.86)
H_2L^{1d}	[H_2sal4-DPS]	62	270	68.12	4.22	6.43
	$C_{26}H_{20}N_2O_4S_1$			(68.42)	(4.38)	(6.14)
H_2L^{2a}	[H_2naphDPM]	56	262	83.01	5.13	5.59
	$C_{35}H_{26}N_2O_2$			(83.00)	(5.13)	(5.53)
H_2L^{2d}	[H_2naph4-DPS]	64	295	73.40	4.21	5.10
	$C_{34}H_{24}N_2O_4S_1$			(73.28)	(4.32)	(5.03)
H_2L^{3a}	[H_2vanDPM]	65	198	74.86	5.74	5.85
	$C_{29}H_{26}N_2O_4$			(74.67)	(5.57)	(6.00)
H_2L^{3d}	[H_2van4-DPS]	60	250	64.35	4.44	7.46
	$C_{28}H_{24}N_2O_6$			(65.11)	(4.65)	(7.42)
H_2L^{4a}	[H_2BrsalDPM]	96	290	57.90	3.80	4.95
	$C_{27}H_{20}N_2O_2Br_2$			(57.45)	(3.54)	(4.96)
H_2L^{4d}	[H_2Brsal4-DPS]	96	307	51.31	3.06	4.43
	$C_{26}H_{18}N_2O_4S_1Br_2$			(50.81)	(2.93)	(4.56)

* Values given in parentheses are calculated from molecular formulae.

2.2.4 Preparation of the $[Cu_2L_2]$, complexes:

2.2.4.1 Preparation of $[Cu_2(salDPM)_2]$:

Ligand [H_2salDPM] (0.507g, 1.25 mmol) was suspended in 30 ml of methanol in a 150 ml flask equipped with a reflux condenser. A solution of cupric acetate monohydrate (0.249g, 1.25 mmol) in 20 ml methanol was added slowly to the above solution. The resulting solution was stirred for three hours at 60 °C. The dark brown coloured microcrystalline solid obtained at the end of reaction was filtered and washed thoroughly with methanol till the washings were clear. The product was dried at 80 °C.

Complexes $[Cu_2(salDPE)_2]$, $[Cu_2(sal4\text{-}DPS)_2]$, $[Cu_2(BrsalDPM)_2]$, $[Cu_2(Brsal4\text{-}DPS)_2]$, $[Cu_2(vanDPM)_2]$, $[Cu_2(van4\text{-}DPS)_2]$, $[Cu_2(naphDPM)_2]$ and $[Cu_2(naph4\text{-}DPS)_2]$ were synthesised using similar procedure as for $[Cu_2(salDPM)_2]$ and appropriate quantities of ligands. (**Scheme 2.2).**

2.2.4.2 Preparation of the complex $[Cu_2(sal3\text{-}DPS)_2]$:

Cupric acetate monohydrate (0.499 g, 2.5 mmol) was dissolved in 30 ml methanol in a flask equipped with a reflux condenser. A solution of 2-hdroxybenzaldehyde (0.611 g, 5 mmol) in 15 ml methanol was added to this. The colour of the solution turned green on coordination of the aldehyde with Cu (II). A solution of 3,3'-diaminodiphenylsulphone (0.621 g, 2.5 mmol) in 20 ml methanol, was added dropwise to the above solution over two hours at reflux temperature. The resulting solution was allowed to reflux for additional one hour with constant stirring. The dark brown microcrystalline solid formed was filtered, washed thoroughly with 30 ml methanol in 5-6 ml portions and dried in air.

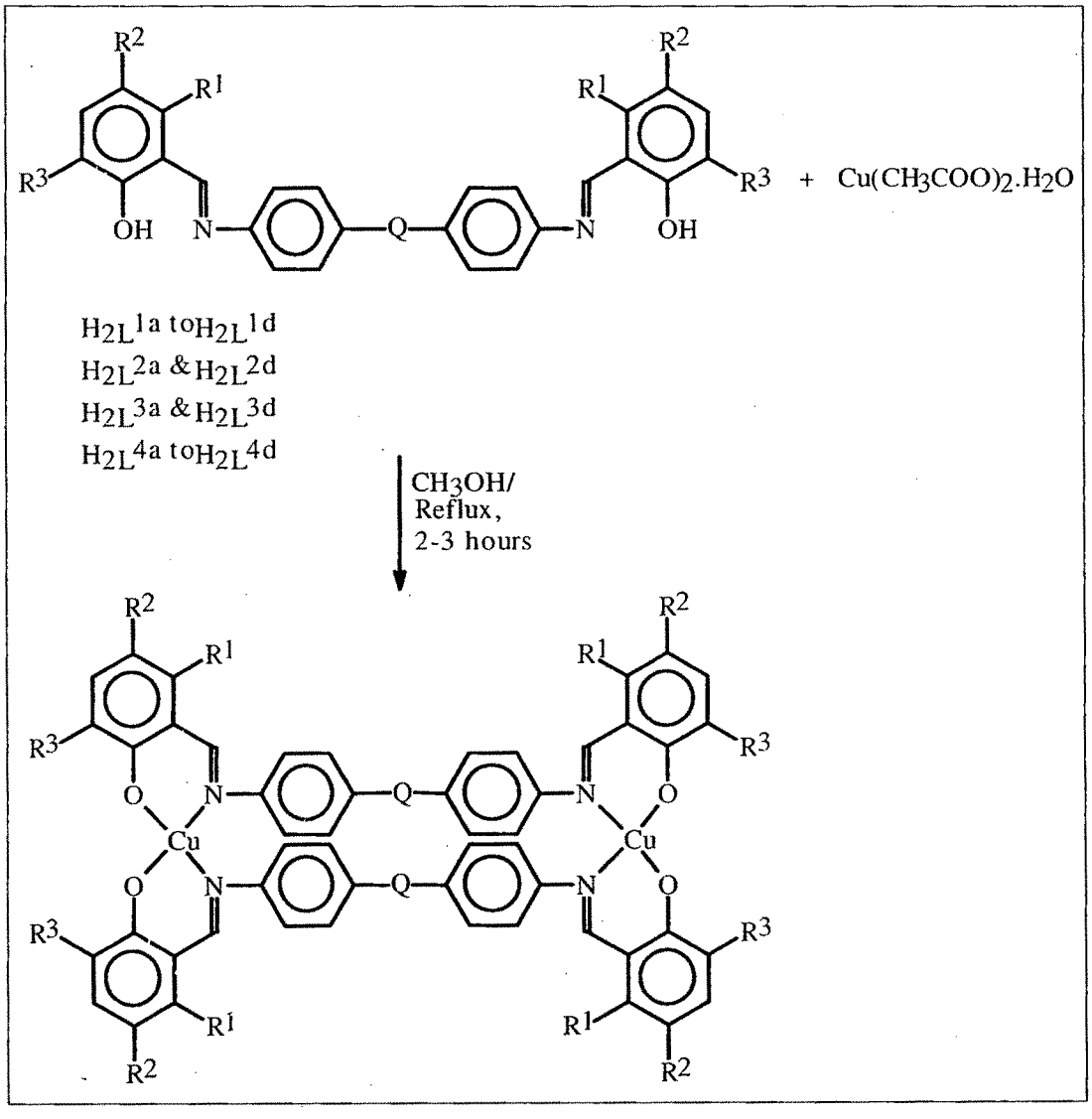

2-I to 2-IV : $R^1 = H, R^2 = H, R^3 = H.$

2-V & 2-VI : $R^1R^2 = -(CH=CH)^2-, R^3 = H.$

2-VII & 2-VIII : $R^1 = H, R^2 = H, R^3 = -OCH_3.$

2-IX & 2-X : $R^1 = H, R^2 = Br, R^3 = H.$

2-I, 2-V, 2-VII, 2-IX : $Q = -CH_2-.$

2-II : $Q = -O-.$

2-III, 2-IV, 2-VI, 2-VIII, 2- X : $Q = -SO_2-.$

[Scheme- 2.2]

2.3 Results and discussion:

Characterization of the binucleating ligands and complexes:

The binucleating Schiff base ligands except those of 3,3'-diaminodiphenylsulphone were obtained in appreciably good yields. The formation of these molecules is confirmed by the absence of $\nu_{>C=O}$ and ν_{NH} as in the original reactants and the appearance of $\nu_{>C=N}$. The IR spectra of the ligands have all other expected features (**Fig. 2.5a** to **Fig. 2.13a**). The melting points and analytical data of these ligands is summarised in **Table-2.1.** The analytical data is agreeable with the calculated values.

The ligand, bis{4-(2-hydroxybenzyl)iminophenyl}ether, (H_2salDPE) was characterised by ^{1}H NMR and ^{13}C NMR in $CDCl_3$. The spectrum is shown in **Fig. 2.2** and **Fig. 2.3**. The proton NMR of the ligands has two multiplets in the regions 6.9 to 7.1 δ and 7.25 to 7.41 δ corresponding to 8 protons each. The multiplet between 6.9 to 7.1 δ can be assigned to the aromatic protons in the hydroxyl phenyl part i.e. H2, H3, H4 and H5. The quartet pattern between 7.25 to 7.41 δ can be assigned to H9 and H10 in diphenyl ether part of the ligand. A singlet due to two –N=CH- protons appears at 8.63 δ. Another singlet corresponding to two phenolic –OH protons appears at 13.97 δ.

In the ^{13}C NMR of the ligand, the lines observed at (δ): 118.090, 119.889, 120.657, 123.565, 132.787, 133.919 and 162.694 correspond to C_4, C_2, C_5, C_3, C_{10} and C_9, respectively. Tertiary carbon, C_1, C_6, C_8 and C_{11}, could not be seen in the spectrum due to weak intensities.

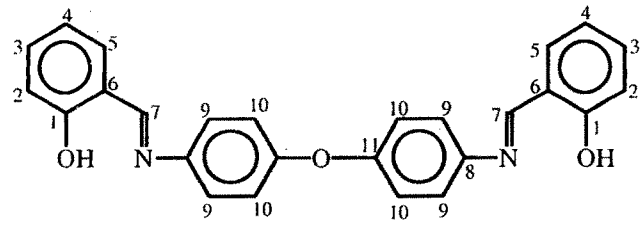

(Binucleating ligand, bis{4-(2-hydroxybenzyl)iminophenyl}ether).

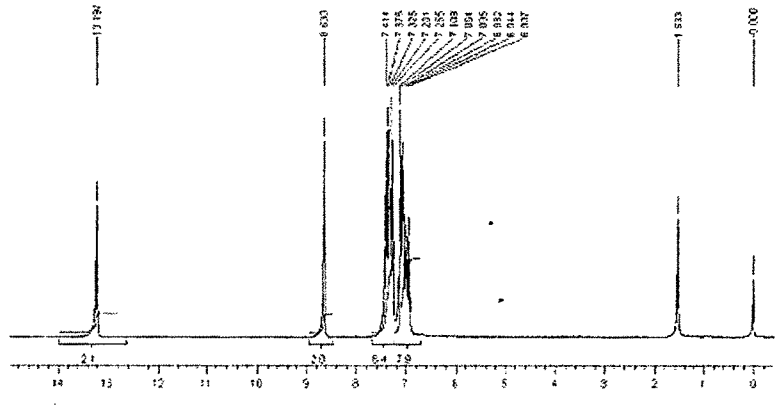

Fig.2.2 ^{1}H NMR, of bis{4-(2-hydroxybenzyl)iminophenyl}ether.

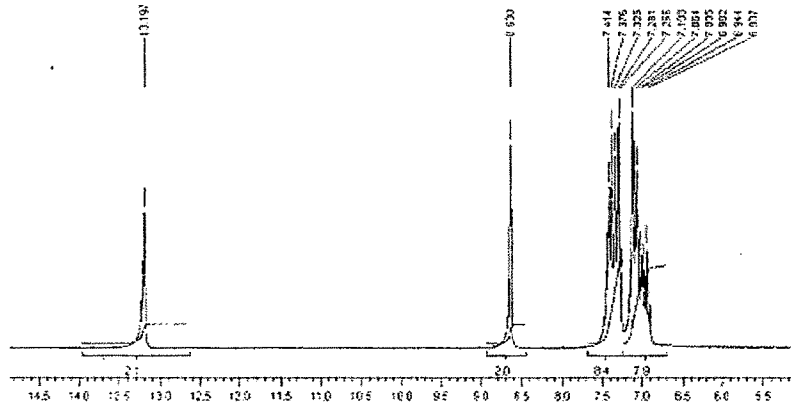

Fig.2.2.1 ^{1}H NMR, of bis{4-(2-hydroxybenzyl)iminophenyl}ether (expanded).

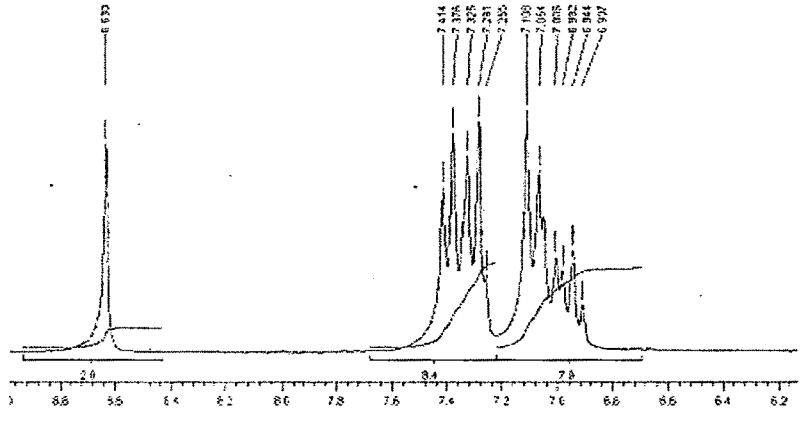

Fig.2.2.2 ^{1}H NMR, of bis{4-(2-hydroxybenzyl)iminophenyl}ether (expanded).

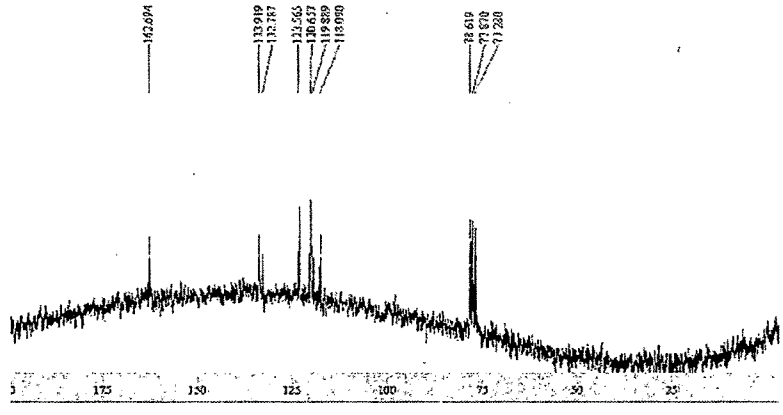

Fig.2.3 ^{13}C NMR, bis{4-(2-hydroxybenzyl)iminophenyl}ether.

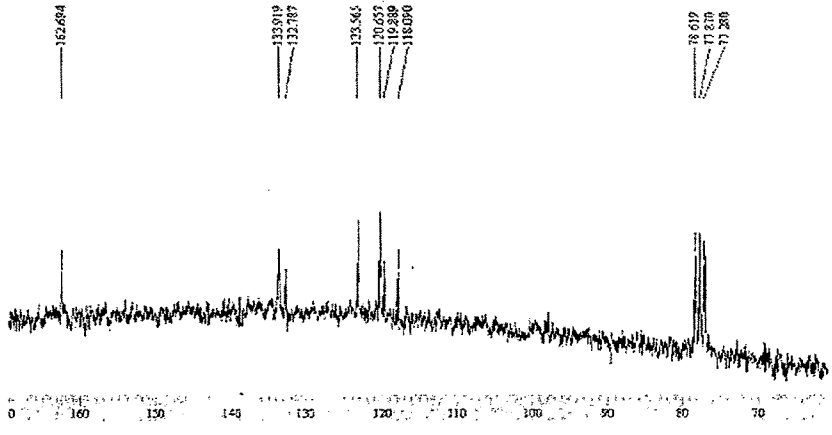

Fig.2.3.1 ^{13}C NMR, bis{4-(2-hydroxybenzyl)iminophenyl}ether (expanded).

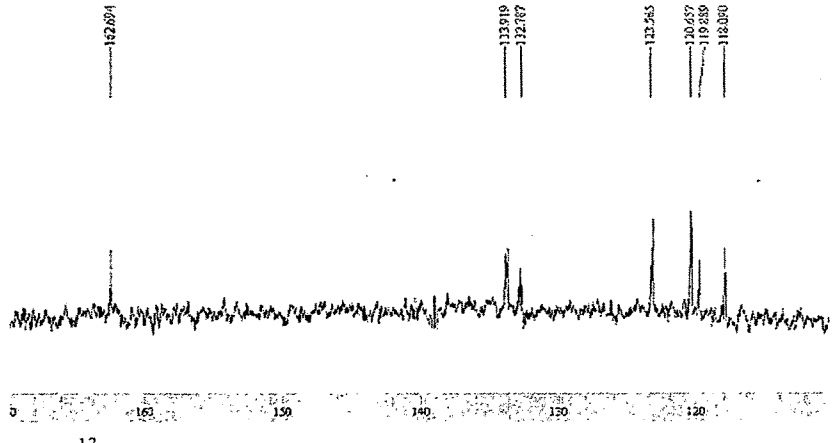

Fig.2.3.2 ^{13}C NMR, bis{4-(2-hydroxybenzyl)iminophenyl}ether (expanded).

The reactions of these ligands in equivalent amounts with cupric acetate monohydrate, as detailed in the earlier section, resulted in the formation of binuclear complexes. 3,3'-Diaminodiphenylsulphone is much less reactive as compared to the diamines used in this work. The condensation with aldehydes was very difficult. Hence, metal assisted synthesis was attempted. The reaction of 3,3'-diaminodiphenylsulphone with $Cu(sal)_2$ and related complexes with 2-hydroxyaromatic carbonyls resulted in the formation of binuclear complexes in appreciable yields.

The elemental analysis of the complexes as summarised in the **Table 2.2,** indicated that the complexes have general formula, $[Cu_2L_2]$. The analytical data also indicates the presence of water molecules in $[Cu_2(salDPM)_2].4H_2O$, $[Cu_2(salDPE)_2].H_2O$, $[Cu_2(sal3\text{-}DPS)_2].3H_2O$, $[Cu_2(sal4\text{-}DPS)_2].2H_2O$ and $[Cu_2(vanDPM)_2].H_2O$ complexes.

Thermo-gravimetric analysis of these complexes **2-I** to **2-IV** and **2-VII** was carried out between the temperature range 50 °C – 800 °C. The loss of water is observed in the temperature range 150 °C – 250 °C corresponds to one to four water molecules as shown in **Table 2.2.** Thus the metal complexes can be formulated as $[Cu_2(salDPM)_2].4H_2O$, $[Cu_2(salDPE)_2].H_2O$, $[Cu_2(sal3\text{-}DPS)_2].3H_2O$, $[Cu_2(sal4\text{-}DPS)_2].2H_2O$ and $[Cu_2(vanDPM)_2].H_2O$. Loss of water at such high temperature indicates that the water molecules are coordinated and not lattice held.

Table 2.2: Preparative yield, analytical data and TGA data of the binuclear complexes.

Comp. No.	Complexes	Yield (%)	Elemental analysis Found (Calc)* C%	H%	N%	Temp. Range (°C)	% wt loss of H_2O
2-I	$[Cu_2(salDPM)_2].4H_2O$	93	65.86	4.81	5.72	180 - 250	7.21
	$C_{54}H_{48}N_4O_8Cu_2$		(64.35)	(4.77)	(5.56)		(7.12)
2-II	$[Cu_2(salDPE)_2].H_2O$	96	64.87	4.13	5.82	180 - 250	1.88
	$C_{52}H_{38}N_4O_7Cu_2$		(65.19)	(3.97)	(5.85)		(1.67)
2-III	$[Cu_2(sal3\text{-}DPS)_2].3H_2O$	83	58.35	3.68	5.22	180 - 280	4.82
	$C_{52}H_{42}N_4O_{11}S_2Cu_2$		(57.29)	(3.86)	(5.14)		(4.95)
2-IV	$[Cu_2(sal4\text{-}DPS)_2].2H_2O$	98	58.28	3.69	5.30	150 - 200	3.00
	$C_{52}H_{40}N_4O_{10}S_2Cu_2$		(58.26)	(3.73)	(5.22)		(3.36)
2-V	$[Cu_2(naphDPM)_2]$	96	73.54	4.34	5.20		-
	$C_{70}H_{48}N_4O_4Cu_2$		(74.00)	(4.23)	(4.93)		
2-VI	$[Cu_2(naph4\text{-}DPS)_2]$	93	65.69	3.55	4.08		-
	$C_{68}H_{44}N_4O_8S_2Cu_2$		(66.07)	(3.56)	(4.53)		
2-VII	$[Cu_2(vanDPM)_2].H_2O$	48	63.70	4.59	5.13	150 - 210	1.88
	$C_{58}H_{50}N_4O_9Cu_2$		(64.86)	(4.65)	(5.22)		(1.67)
2-VIII	$[Cu_2(van4\text{-}DPS)_2]$	59	58.06	3.92	4.50		-
	$C_{56}H_{44}N_4O_{12}S_2Cu_2$		(58.17)	(3.80)	(4.84)		
2-IX	$[Cu_2(BrsalDPM)_2]$	98	51.11	3.23	4.53		-
	$C_{54}H_{36}N_4O_4Br_4Cu_2$		(51.81)	(2.87)	(4.47)		
2-X	$[Cu_2(Brsal4\text{-}DPS)_2]$	96	46.87	2.35	3.84		-
	$C_{52}H_{32}N_4O_8Br_4S_2Cu_2$		(46.20)	(2.37)	(4.14)		

*Values given in parentheses are calculated from the molecular formulae.

2.3.1. Electronic spectra:

The electronic spectra of the binuclear complexes in methanolic solutions show bands in the range of 276 to 404 nm. The bands in the region 276 - 404 nm agree with the bands observed in the free ligands. Some of these bands are slightly shifted towards lower energy region compared to the free ligand transitions because of the coordination with the metal ion. The bands between 380 - 430 nm can be assigned to the MLCT transition from copper (II) ion to the imine nitrogen atoms.

The complexes $[Cu_2(naphDPM)_2]$ and $[Cu_2(naph4\text{-}DPS)_2]$ do not have appreciable solubility in methanol or any non coordinating solvent. Hence, the intra ligand charge transfer and ligand field transitions could not be seen in the solution spectra. However, the transitions are clearly observed in the diffuse reflectance spectra in the powder form recorded using $BaSO_4$ as reference material (**Table 2.3**).

Table 2.3: Electronic spectral properties of binuclear complexes.

Complexes	**Absorption in methanolic solutions (λ in nm)**	**d.r.s. (λ in nm)**
$[Cu_2(salDPM)_2].4H_2O$	390 & 276	700
$[Cu_2(salDPE)_2].H_2O$	390& 298	810
$[Cu_2(sal3\text{-}DPS)_2].3H_2O$	386 & 292	666
$[Cu_2(sal4\text{-}DPS)_2].2H_2O$	338 & 294	670
$[Cu_2(naphDPM)_2]$	-	426 & 710
$[Cu_2(naph4\text{-}DPS)_2]$	-	418 & 722
$[Cu_2(vanDPM)_2].H_2O$	508, 404& 308	720
$[Cu_2(van4\text{-}DPS)_2]$	398 & 298	740
$[Cu_2(BrsalDPM)_2]$	394 & 298	658
$[Cu_2(Brsal4\text{-}DPS)_2]$	394& 296	720

The diffuse reflectance spectra of the complexes exhibit the ligand field transitions between 650 to 810 nm regions. The broad bands observed in all the complexes are characteristic of d^9 metal ions in square planar geometry. The single broad band in each complex is a combination of the three possible transitions $A_{1g} \leftarrow B_{1g}$, $B_{2g} \leftarrow B_{1g}$ and $E_{1g} \leftarrow B_{1g}$.

2.3.2 IR spectra:

The IR spectra of the complexes (**Fig. 2.5b** to **Fig. 2.13b, Table 2.4**) in the 400 cm^{-1} – 4000 cm^{-1} region exhibit several bands corresponding to stretching and bending of -C–C-, –C–H-, >C=N- etc.

The important IR features, however, are those associated with >C=N- stretching (condensation of aldehydes with diamine to form Schiff base).

A strong absorption appears between 1600cm^{-1} - 1612 cm^{-1} region in all the complexes. This can be attributed to the >C=N- stretching. These vibrations occur at lower frequencies compared to the $\nu_{>C=N-}$ in free ligands where they appear between 1616 cm^{-1} – 1624 cm^{-1} (**Fig. 2.5a to Fig. 5.13a**). The shift towards lower energy in the complexes indicates direct involvement of the imine nitrogen in the coordination to the metal ion. A broad band appears in the in 3600 cm^{-1} - 3200 cm^{-1} in $[Cu_2(salDPM)_2]$, $[Cu_2(salDPE)_2]$, $[Cu_2(sal4\text{-}DPS)_2]$, $[Cu_2(sal3\text{-}DPS)_2]$ and $[Cu_2(vanDPM)_2]$. This corresponds to ν_{-OH}. The presence of this band supports the presence of water molecules in the complexes.

The characteristic asymmetric stretchings band corresponding to ν_{-CH2-}, ν_{-SO2-} and ν_{C-O-C} in the ligands appear at 2924 cm^{-1} – 2928 cm^{-1}, 1358 cm^{-1} – 1379 cm^{-1} and 1027 cm^{-1}, respectively. Other characteristic features of the ligands observed in the IR spectra of both, the ligands and the complexes include –C=C– stretching in aromatic ring between 1590 cm^{-1} – 1490 cm^{-1}, stretching of the phenolic group ν_{-C-O} between 1260 cm^{-1} – 1180 cm^{-1} and ν_{-OCH3} at 1238 cm^{-1} in the complexes derived from

vanillin (**Table 2.4**), the corresponding bending vibrations are observed in 600 – 900 cm^{-1} region.

Table 2.4: Important IR frequencies (cm^{-1}) of the binucleating Schiff base ligands and binuclear complexes.

Complexes	$\nu_{>C=N-}$* (cm^{-1})	*Miscellaneous frequencies* (cm^{-1})
$[H_2salDPM]$	1619	ν_{-CH2-} 2923
$[Cu_2(salDPM)_2.].4H_2O$	1612	ν_{-CH2-} 2924
$[H_2salDPE]$	1620	ν_{-O-} 1032
$[Cu_2(salDPE)_2].H_2O$	1609	ν_{-O-} 1027
$[Cu_2(sal3\text{-}DPS)_2].3H_2O$	1609	ν_{-SO2-} 1357
$[H_2sal4\text{-}DPS]$	1618	ν_{-SO2-} 1368
$[Cu_2(sal4\text{-}DPS)_2].2H_2O$	1609	ν_{-SO2-} 1357
$[H_2naphDPM]$	1624	ν_{-CH2-} 2921
$[Cu_2(naphDPM)_2]$	1600	ν_{-CH2-} 2922
$[H_2naph4\text{-}DPS]$	1624	ν_{-SO2-} 1352
$[Cu_2(naph4\text{-}DPS)_2]$	1602	ν_{-SO2-} 1342
$[H_2vanDPM]$	1618	ν_{-CH2-} 2924, $\nu_{-C\text{-}O\text{-}CH3}$ 1253
$[Cu_2(vanDPM)_2].H_2O$	1612	ν_{-CH2-} 2928, $\nu_{-C\text{-}O\text{-}CH3}$ 1239
$[H_2van4\text{-}DPS]$	1618	ν_{-SO2-} 1374, $\nu_{-C\text{-}O\text{-}CH3}$ 1253
$[Cu_2(van4\text{-}DPS)_2]$	1608	ν_{-SO2} 1334, $\nu_{-C\text{-}O\text{-}CH3}$ 1238
$[H_2BrsalDPM]$	1618	ν_{-CH2-} 2924, $\nu_{-C\text{-}Br}$ 628
$[Cu_2(BrsalDPM)_2]$	1608	ν_{-CH2-} 2926, $\nu_{-C\text{-}Br}$ 645
$[H_2Brsal4\text{-}DPS]$	1616	ν_{-SO2-} 1388, $\nu_{-C\text{-}Br}$ 651
$[Cu_2(Brsal4\text{-}DPS)_2]$	1602	ν_{-SO2-} 1379, $\nu_{-C\text{-}Br}$ 658

*The shift in the $\nu_{>C=N-}$ stretching towards lower energy is due to the coordination of nitrogen with Copper (II).

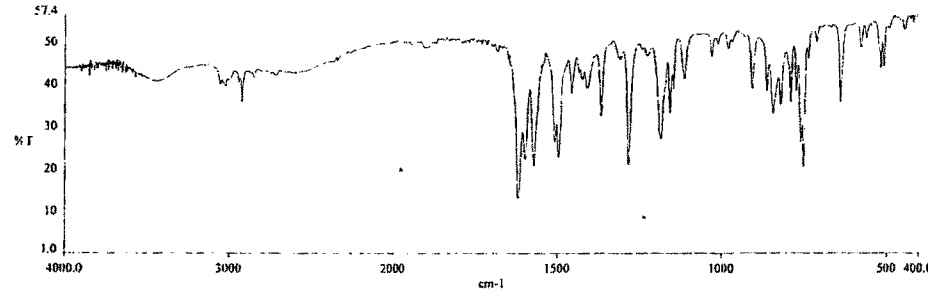

Fig. 2.5a FTIR spectrum of the binucleating ligand, [H_2salDPM]

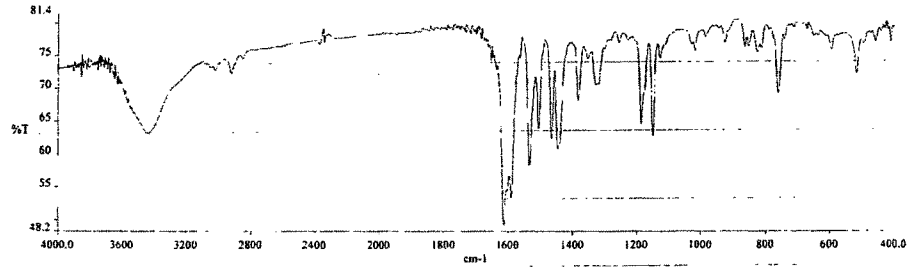

Fig. 2.5b FTIR spectrum of the binuclear complex [Cu_2(salDPM)$_2$.]4H_2O.

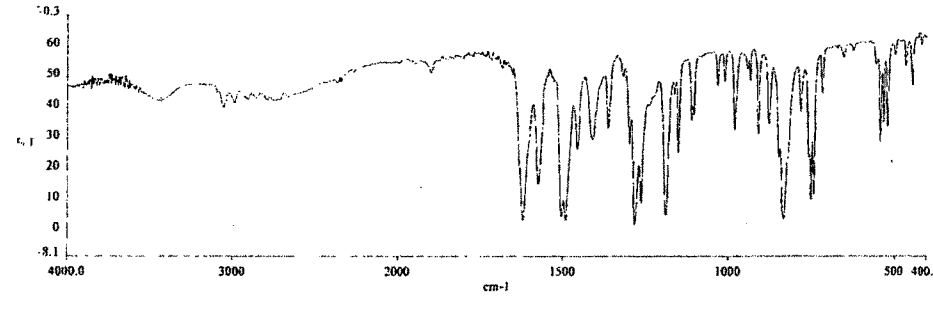

Fig. 2.6a FTIR spectrum of the binucleating ligand, [H_2salDPE]

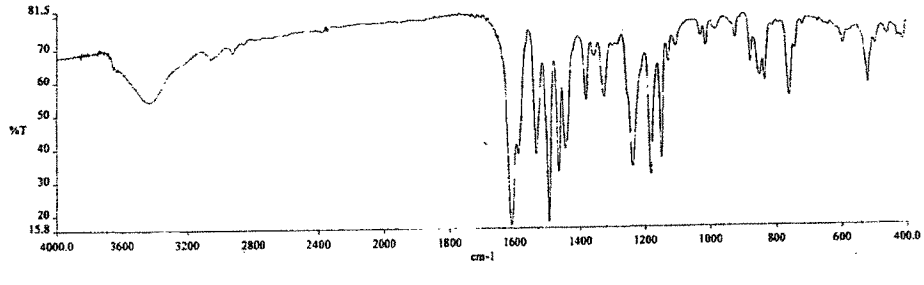

Fig. 2.6.b FTIR spectrum of the binuclear complex [Cu_2(salDPE)$_2$].H_2O.

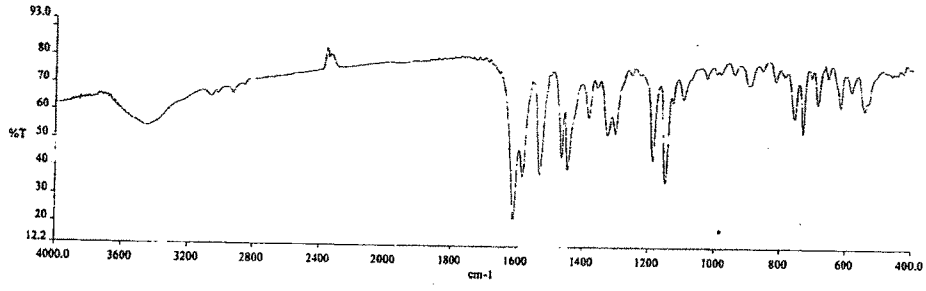

Fig. 2.7a FTIR spectrum of binuclear complex $[Cu_2(sal3\text{-}DPS)_2].3H_2O$

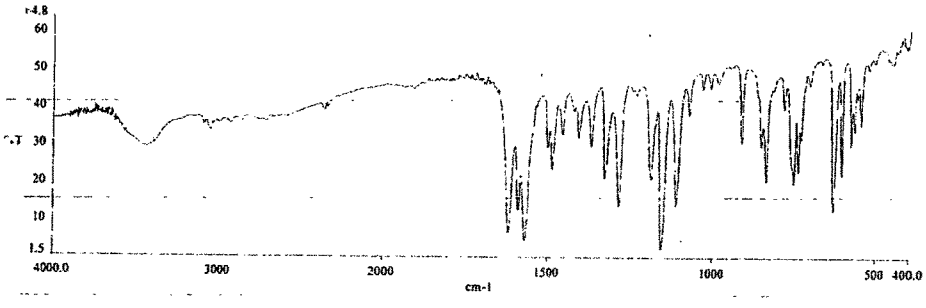

Fig. 2.7b FTIR spectrum of the binucleating ligand, $[H_2sal4\text{-}DPS]$

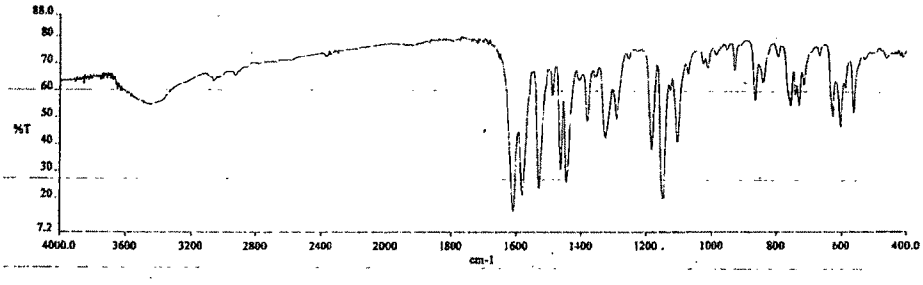

Fig. 2.7b IR spectrum of the binuclear complex $[Cu_2(sal4\text{-}DPS)_2].2H_2O$

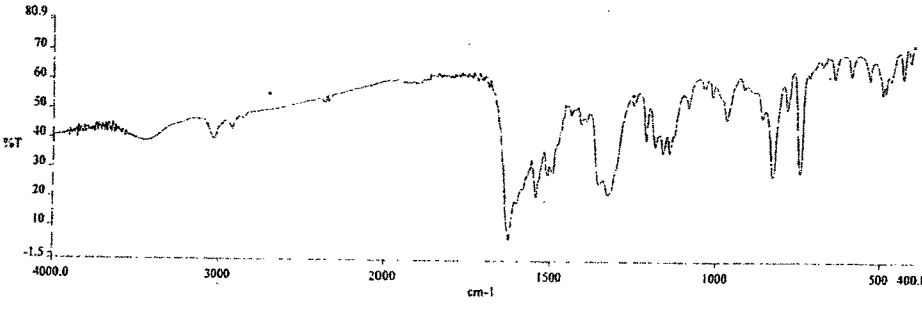

Fig. 2.8a FTIR spectrum of the binucleating ligand, $[H_2naphDPM]$

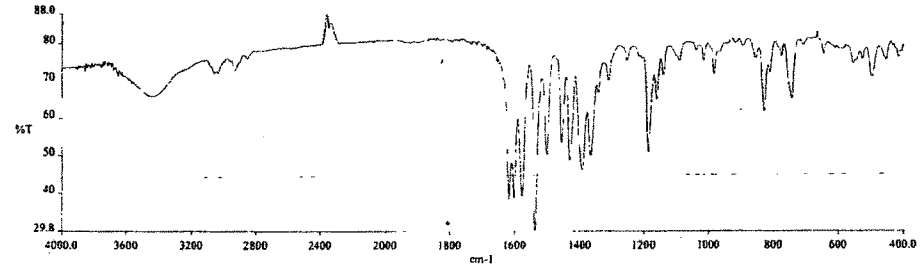

Fig. 2.8b IR spectrum of the binuclear complex $[Cu_2(naphDPM)_2]$.

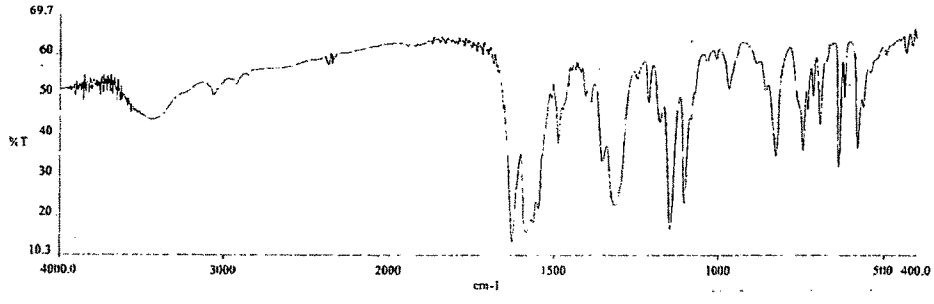

Fig. 2.9a FTIR spectrum of the binucleating ligand, $[H_2naph4\text{-}DPS]$.

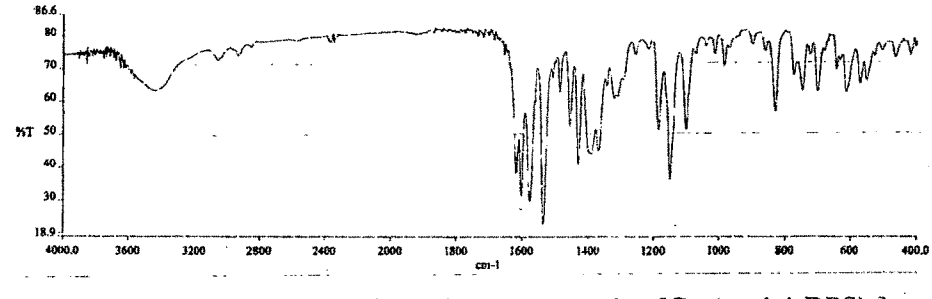

Fig. 2.9b FTIR spectrum of the binuclear complex $[Cu_2(naph4\text{-}DPS)_2]$.

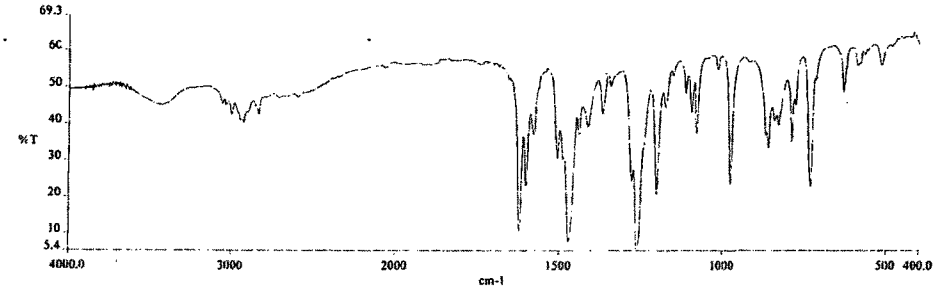

Fig. 2.10a FTIR spectrum of the binucleating ligand, $[H_2vanDPM]$

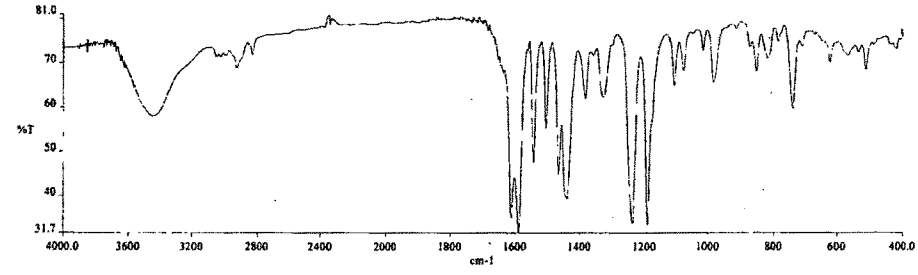

Fig. 2.10b FTIR spectrum of the binuclear complex $[Cu_2vanDPM)_2].H_2O$.

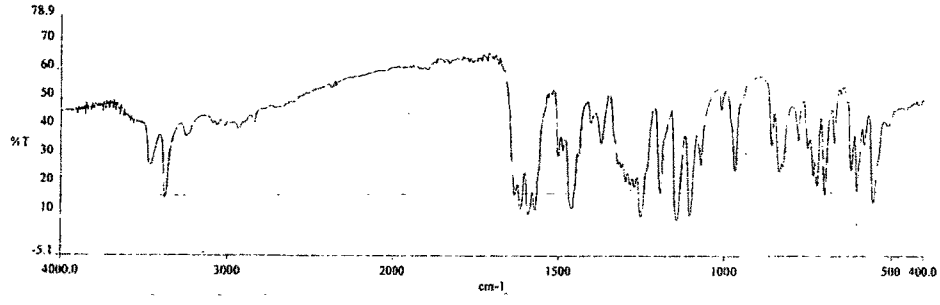

Fig. 2.11a FTIR spectrum of the binucleating ligand, $[H_2van4\text{-}DPS]$.

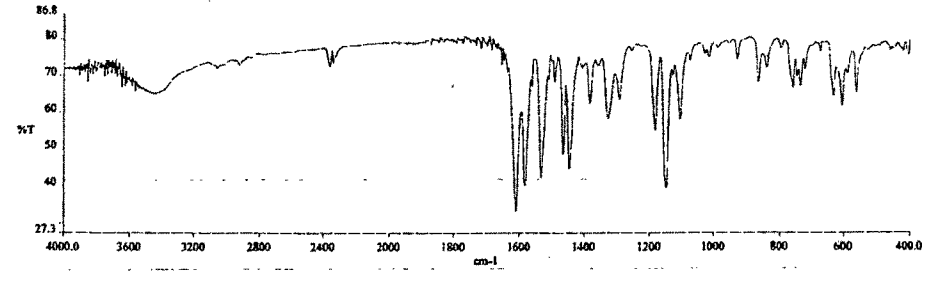

Fig. 2.11b FTIR spectrum of the binuclear complex $[Cu_2(vanDPS)_2]$.

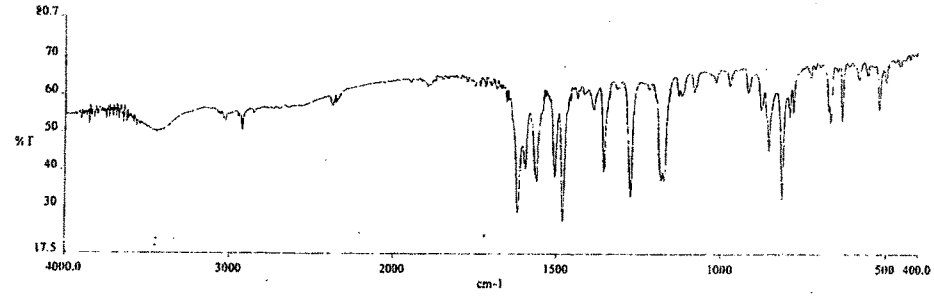

Fig. 2.12a FTIR spectrum of the binucleating ligand, $[H_2BrsalDPM]$

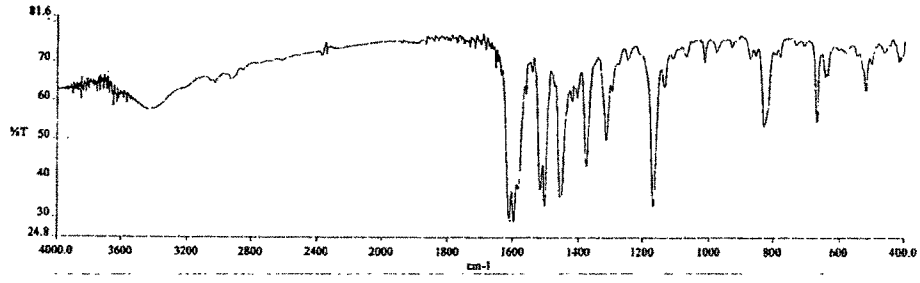

Fig.2.12b FTIR spectrum of the binuclear complex $[Cu_2(BrsalDPM)_2]$.

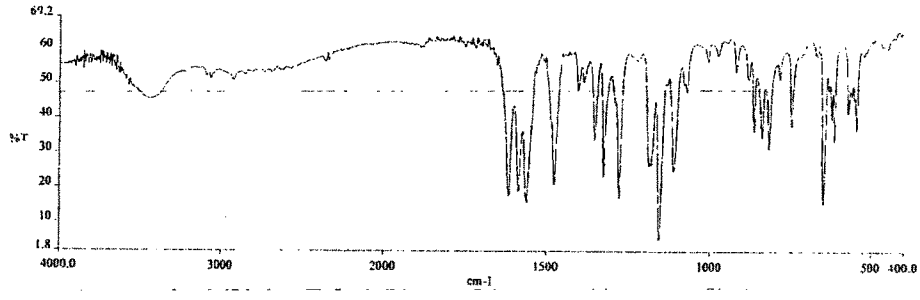

Fig. 2.13a FTIR spectrum of the binucleating ligand, $[H_2Brsal4\text{-}DPS]$.

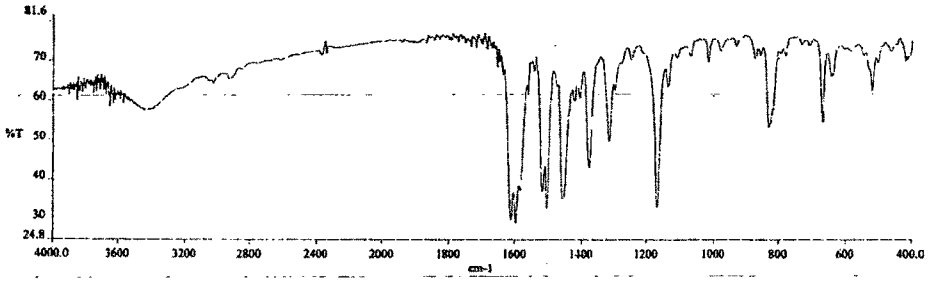

Fig.2.13b FTIR spectrum of the binuclear complex $[Cu_2(Brsal4\text{-}DPS)_2]$.

2.3.3 Mass Spectra:

The FAB mass spectrum of the complex $[Cu_2(BrsalDPM)_2]$ (**Fig. 2.14**), consists of a peak corresponding to the parent binuclear mono cation $[Cu_2(BrsalDPM)_2]^+$ at m/z 1250 with relative aboundance value of 65% . The peak corresponding to the parent binuclear dication, $[Cu_2(BrsalDPM)_2]^{2+}$, is observed at m/z 625 with very high relative abundance value 92%. The presence of these peaks confirms the formation of binuclear complexes rather than polynuclear species.

Some of the important fragments are noted in **Table 2.5** and their probable structural formulae are schematized in the following **Fig. 2.14.1.** A peak corresponding to $[Cu_2(BrsalDPM)]^+$ at m/z 690 is observed with relative abundance of 45% . The existence of this fragment supports the bis-bidentate coordination mode of the ligand and hence the formation of binuclear complex. This fragment loses one Cu atom to give a peak corresponding to $[Cu(BrsalDPM)_2]^+$ at m/z 627.

A peak corresponding to free binucleating Schiff base ligand $[(BrsalH)_2DPM)]^+$ appears at m/z 565 (60%) . This species undergoes further fragmentation to give other related species.

The peak corresponding to the fragments of m-nitrobenzyl alcohol and associated products are observed at m/z 136, 137, 154, 289 and 307.These fragments get associated with various fragments of metal complexes and thus are responsible for the occurrence of widely distributed species with high masses and low abundance.

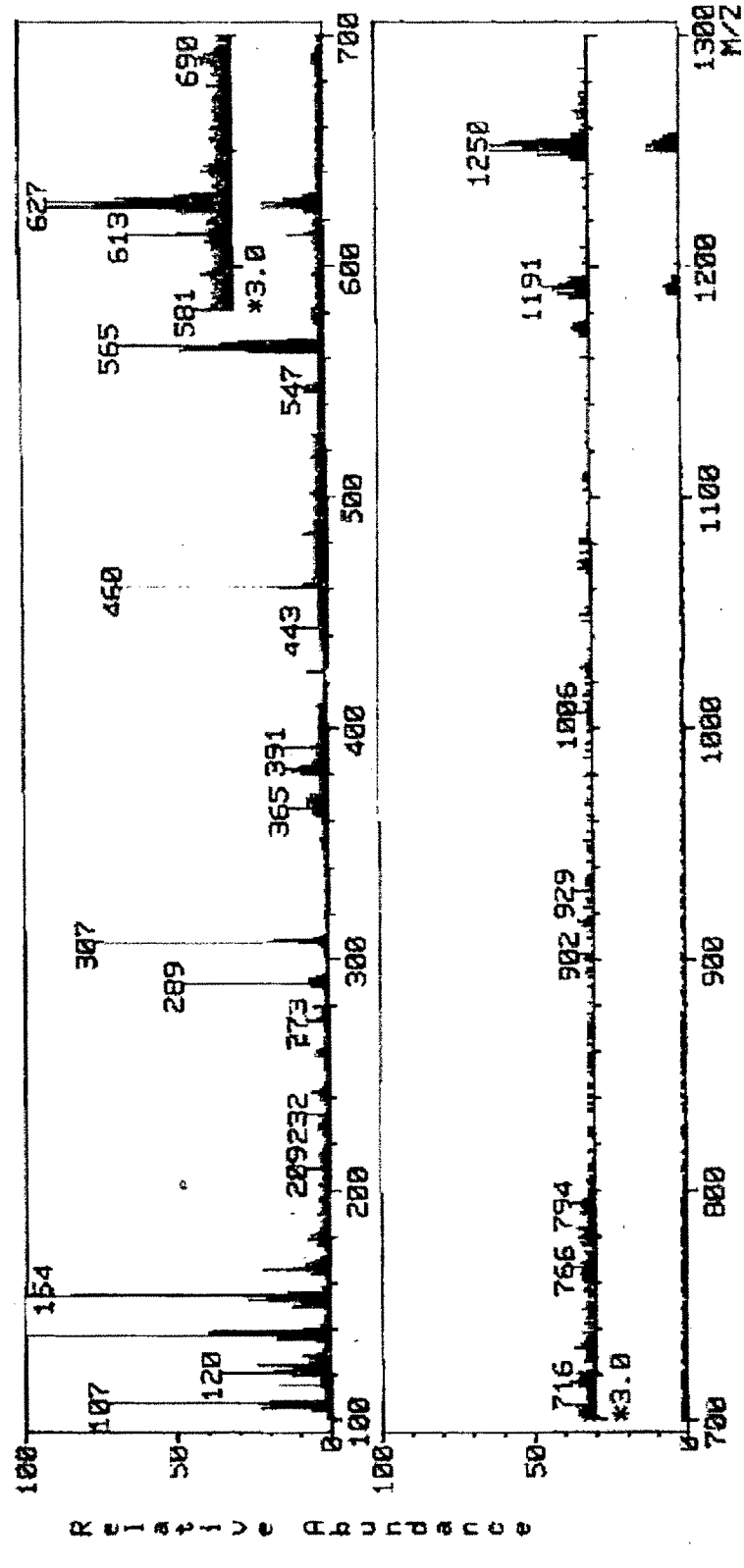

Fig. 2.14 FAB - Mass spectra of $[Cu_2(BrsalDPM)_2]$.

Table: 5.7 Fragmentation pattern in the positive ion FAB-MS of $[Cu_2(BrsalDPM)_2]$ in m-nitrobenzyl alcohol.

m/z (%relative abundance)	Molecular formula
1250 (65%)	$[C_{54}H_{36}O_4N_4Br_4Cu_2]^+$
902 (44%)	$[C_{34}H_{22}O_4N_3Br_3Cu_2]^+$
690 (45%)	$[C_{27}H_{19}O_2N_2Br_2Cu_2]^+$
629 (38%)	$[C_{54}H_{40}O_4N_4Br_4Cu_2]^{2+}$
627 (92%)	$[C_{54}H_{38}O_4N_4Br_4Cu_2]^{2+}$
625 (92%)	$[C_{54}H_{36}O_4N_4Br_4Cu_2]^{2+}$
565 (60%)	$[C_{27}H_{21}O_2N_2Br_2]^+$
547 (5%)	$[C_{27}H_{19}ON_2Br_2]^+$
460 (70%)	$[C_{20}H_{16}ON_2Br_2]^+$
443 (12%)	$[C_{20}H_{15}N_2Br_2]^+$
365 (13%)	$[C_{14}H_9N_2Br_2]^+$
363 (8%)	$[C_{14}H_7N_2Br_2]^+$
120 (18%)	$[C_7H_6NO]^+$
107 (38%)	$[C_7H_7O]^+$

Fig. 2.14.1 Possible structures of $[Cu_2(BrsalDPM)_2]$ and the corresponding fragments in FAB mass.

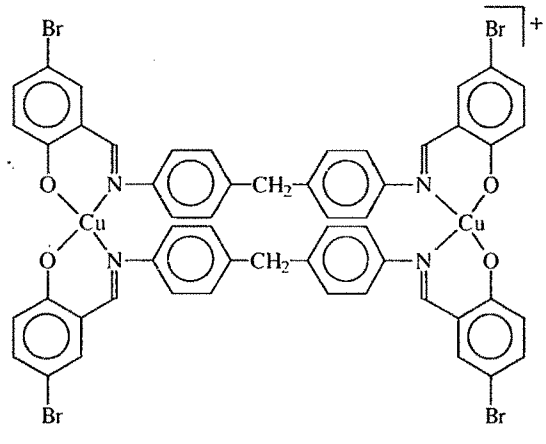

m/z 1250 (65%), $[C_{54}H_{36}O_4N_4Br_4Cu_2]^+$

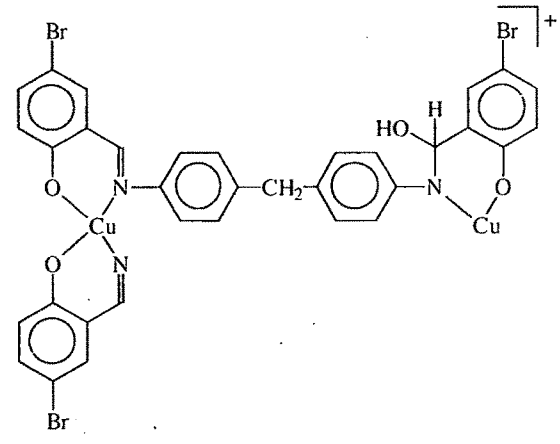

m/z 902 (44%), $[C_{34}H_{22}O_4N_3Br_3Cu_2]^+$

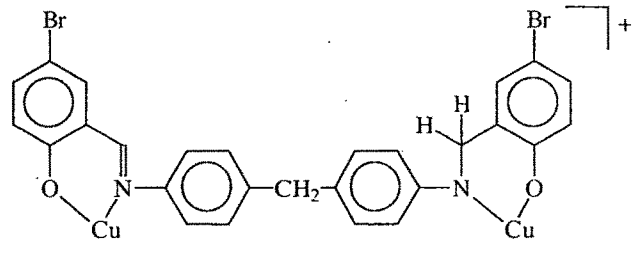

m/z 690(45%), $[C_{27}H_{19}O_2N_2Br_2Cu_2]^+$

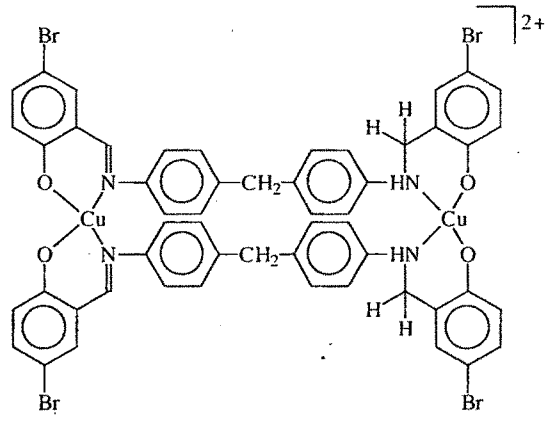

m/z 629(38%) $[C_{54}H_{40}O_4N_4Br_4Cu_2]^{2+}$

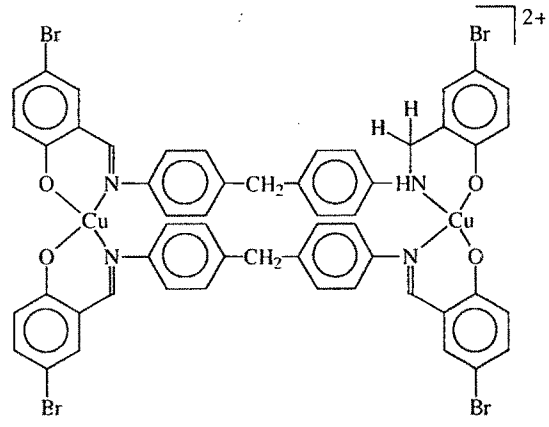

m/z 627(92%) $[C_{54}H_{38}O_4N_4Br_4Cu_2]^{2+}$

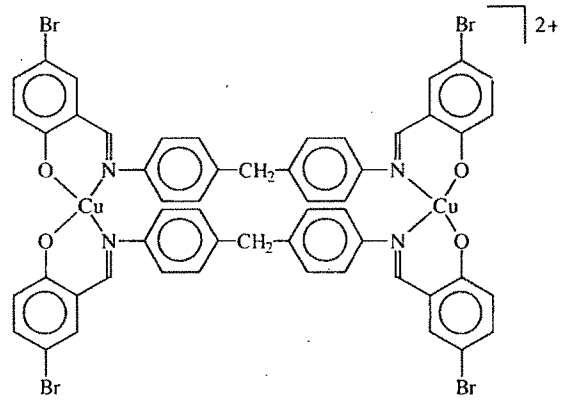

m/z 625 (92%), $[C_{54}H_{36}O_4N_4Br_4Cu_2]^{2+}$

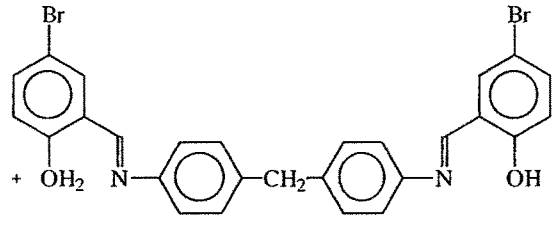

m/z 565(60%), $[C_{27}H_{21}O_2N_2Br_2]^{+}$

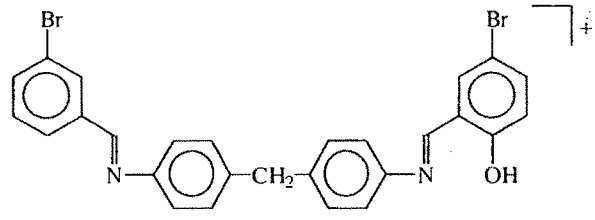

m/z 547(5%), $[C_{27}H_{19}O_1N_2Br_2]^+$

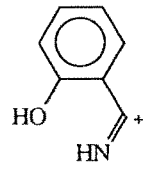

m/z 120 (18%), $[C_7H_6NO]^+$

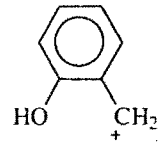

m/z 107 (38%), $[C_7H_7O]^+$

2.3.4 ESR spectra:

The ESR spectra of complex, $[Cu_2(BrsalDPM)_2]$ were recorded at room temperature in polycrystalline powder form and as frozen solution in DMF at LNT. The spectra at RT and LNT are both identical, **Fig. 2.15.** They are typical axial ESR indicating tetragonal distortion / near square planar geometry around copper ion. The $g_{\parallel}$ and $g_{\perp}$ values recorded in **Table 2.6,** are typical of normal copper (II) coordination. A very weak transition at half field strength is also observed indicating the possibility of magnetic exchange between two copper (II) ions.

Table 2.6: ESR of the $[Cu_2(BrsalDPM)_2]$

	$g_{\perp}$	$g_{\parallel}$
Room temperature	2.06001	2.230279
Liquid N_2 temperature	2.05691	2.211886

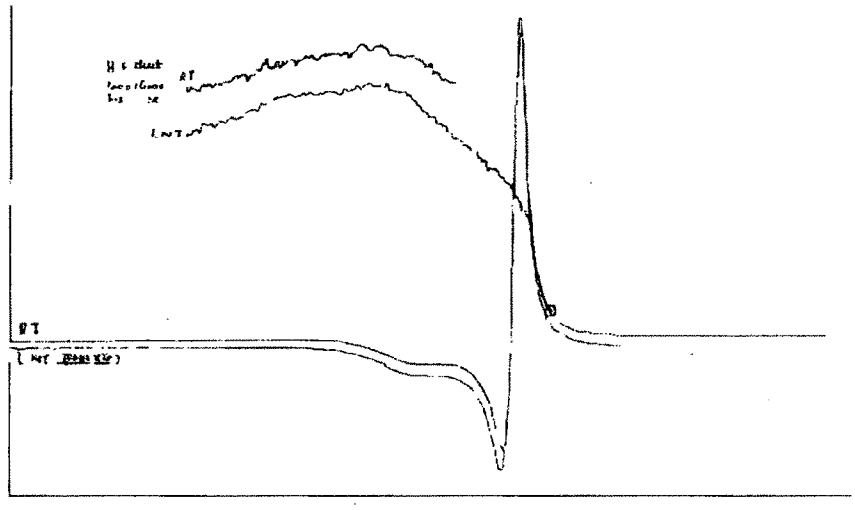

Fig 2.15 ESR of the $[Cu_2(BrsalDPM)_2]$

2.3.5 Magnetic Exchange:

The magnetic susceptibility measurements between 90 °K – 270 °K and the subsequent least squares fit of the experimental data to the Bleaney – Bower's equation were used to evaluate the coupling constant J between the copper (II) centres in the binuclear complexes , **2-I, 2-II, 2-III, 2-IV, 2-V, 2-VII** and **2-IX** . The χ_M vs T plots with calculated and observed values are shown in **Fig. 2.16.1 to Fig. 2.16.5.** The values of J range between -7.24 cm^{-1} to 53.16 cm^{-1}, **(Table 2.7).** As the values indicate, all of the binuclear complexes studied, except $[Cu_2(salDPM)_2]$, have moderately strong ferromagnetic exchange.

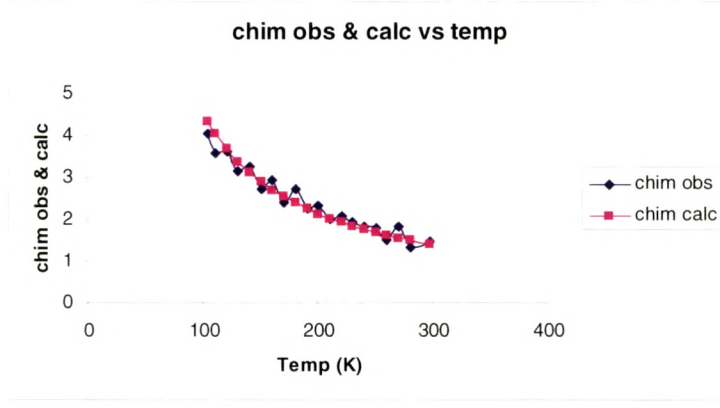

Fig.2.16.1 [Cu_2(salDPE)$_2$]

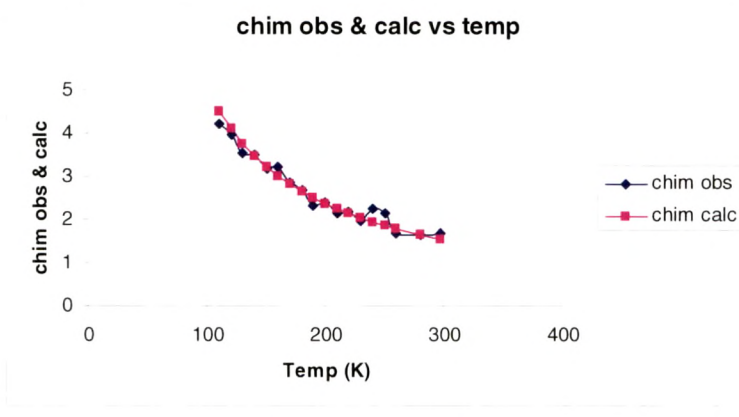

Fig.2.16.2 [Cu_2(sal3DPS)$_2$]

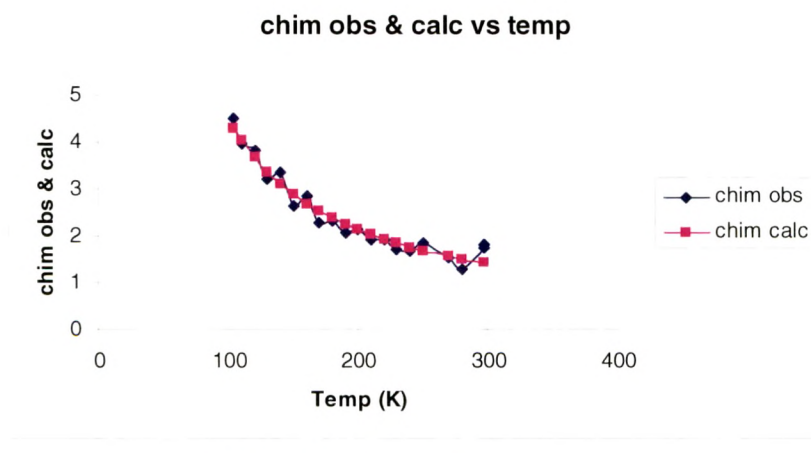

Fig.2.16.3 [Cu_2(naphDPM)$_2$]

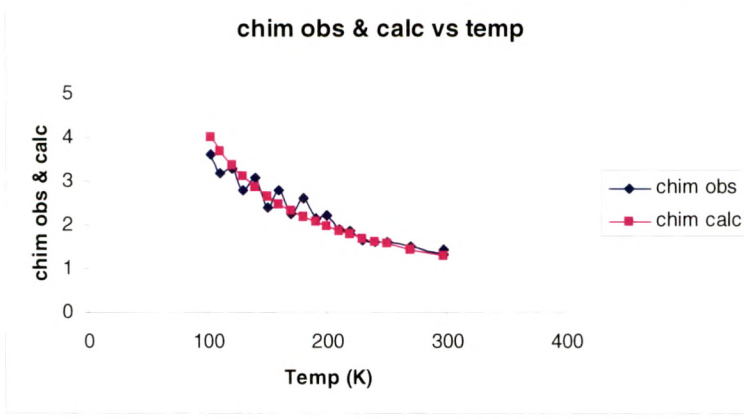

Fig.2.16.4 [Cu_2(vanDPM)$_2$]

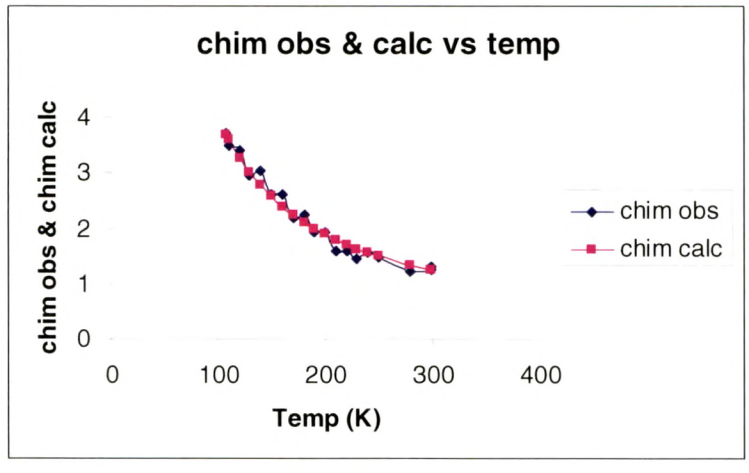

Fig.2.16.5 [Cu_2(BrsalDPM)$_2$]

The magnetic exchange interaction between the paramagnetic metal ions is shown to depend on several parameters related to the geometry of the molecule and energy of the paramagnetic orbitals. The influence of such parameters on the magnetic exchange can be understood by considering ligand mediated interaction between paramagnetic orbitals as illustrated in **Fig. 2.17**

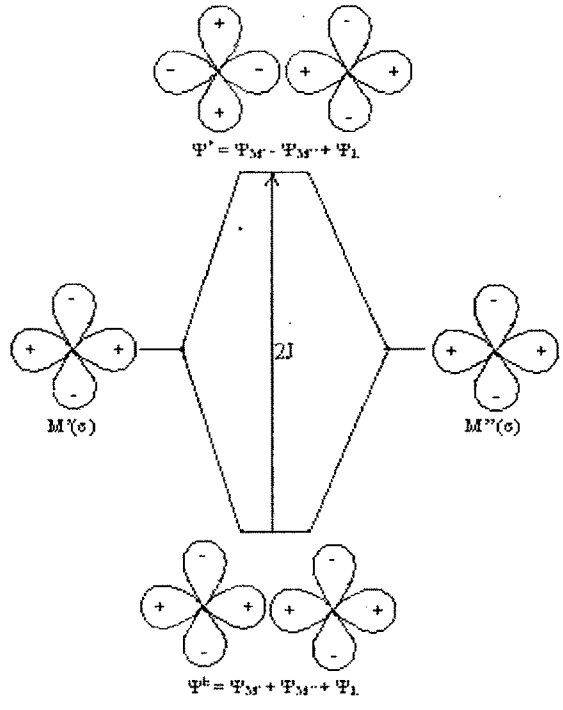

(Fig. 2.17)

The multiatomic bridging ligands, specially those having conjugated π – systems, have a number of closely spaced molecular orbitals. Usually one of these closely spaced orbitals can have matching energy and symmetry with paramagnetic orbitals. The interaction can lead to the formation of two metal centred molecular orbitals one of them essentially bonding and the other essentially antibonding. The paramagnetic orbitals of the metal ion being the highest occupied amongst all interacting orbitals, the resulting MOs are usually the HOMO and the LUMO. The occupation of these two orbitals by the two unpaired electrons over the metal ions leads to the singlet and triplet states with an energy difference of 2J.

If -2J = kT, the magnetic susceptibility depends on Boltazman population distribution, of singlet and triplet state and leads to paramagnetism. However, if -2J>kT the population of singlet state increase and ultimately the system becomes diamagnetic below certain temperature i.e. antiferromagnetism is the result.

The situation, where -2J<kT at all temperature, can arise when there is no effective interaction between the paramagnetic orbitals or the orbital orientation forces them to remain degenerate. In such cases, the ground state is a triplet state and hence the result is ferromagnetism.

The extent of such ligand mediated exchange in binuclear complexes depends on:

(i) the energy of the interacting orbitals and

(ii) the variation in geometrical parameter such as

(a) metal-ligand bond length

(b) M-L-M bridge angle (ϕ)

(c) Dihedral angle between coordination planes, θ and

(d) Degree of planarity of the bridging unit.

Super exchange interaction in the binuclear complexes can be considered as a special case with the interacting bridging MO's being replaced by the bridging atom orbitals. Mckee and Smith [24] studied, binuclear copper (II) complexes, bridged by single alkoxy oxygen. These complexes were shown to have a maximum Cu-O-Cu angle of 135°. The magnetic moment of the complex was found to be 0.6 BM per Cu (II) centre at room temperature, indicating the presence of a strong antiferromagnetic interaction. A number studies [25-32] have shown that in μ-oxo i.e. μ-hydroxo, μ-alkoxo, or μ-phenoxo bridged dicopper (II) complexes the extent of antiferromagnetic exchange decrease with the decrease in the Cu-O-Cu angle ϕ and becomes ferromagnetic below the angle of 97.5°. In addition to the optimum value of the M-L-M angle (ϕ), the planarity of the binuclear core structure is also an important requirement, for the exchange interaction to take place. Kahn et al [33-34] showed the dependence of the value of J on the dihedral angle (θ), between the two copper coordination planes in O-bridged non planar dimers. There is maximum antiferromagnetic interaction between the magnetic orbitals, when the dihedral angle between coordination planes, θ is zero or 180°. Any distortion of the binuclear core structure from the planarity, resulting in increase in dihedral angle, reduces the overlap

of copper (II) d_{x2-y2} orbitals with the bridging oxide ion orbitals, and as a consequence the exchange interaction is weakened.

Thus the existence of a linear relationship between 2J and the bridging angle ϕ or the dependence of spin exchange or the dihedral angle θ is out of the requirement of the maximum extent of interaction between the paramagnetic orbitals through the bridge.

A similar relationship between geometrical parameters and the extent of spin exchange may be expected in the complexes with multiatomic bridging units.

In the complexes reported here, a systematic variation is made in the bridging part of the binucleating ligand. The bis-phenyl moieties are linked by etherial O, methylene $-CH_2-$ or sulphonyl $-SO_2-$. Sulphonyl bridging at 3 or 4 position with respect to the coordinating site has been selected to provide an insight into the effect of positional isomers. The non bridging part of the ligands have substitutions at 3, 4 and 5 positions. These are expected to bring in variation in the electron density over the coordinating atom, its π – bonding ability and hence affect the coordination geometry.

In order to analyse the geometrical parameters in the complexes, the geometry of the complexes were optimised using Universal Force Field [35-36]. The optimised geometry of the complexes is given in **fig. 2.18.1** to **fig. 2.18.7**. The torsional angle between the metal coordination planes were determined and have been correlated with the extent of spin exchange, **Table 2.7**.

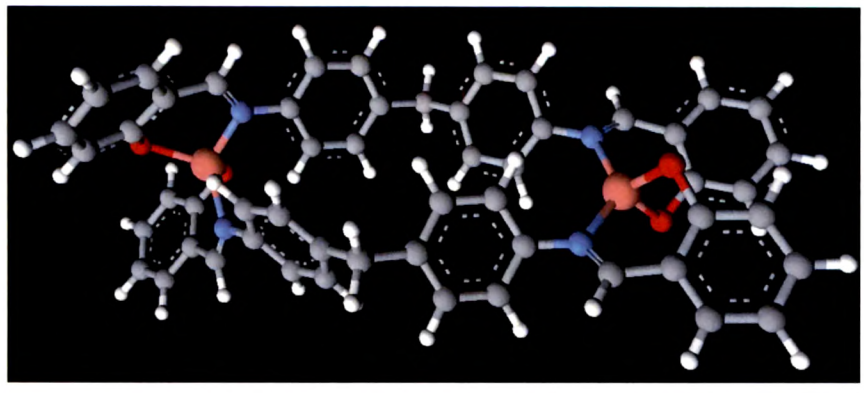

Fig 2.18.1 Optimised geometry of $[Cu_2(salDPM)_2]$

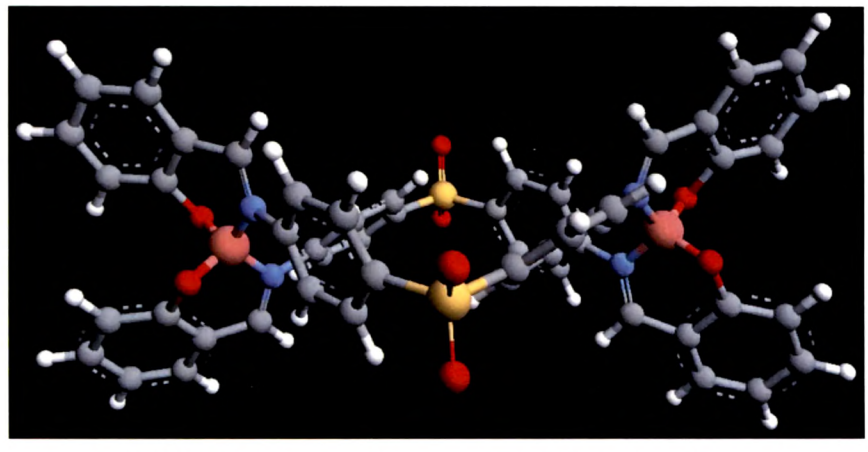

Fig 2.18.2 Optimised geometry of $[Cu_2(sal4\text{-}DPS)_2]$

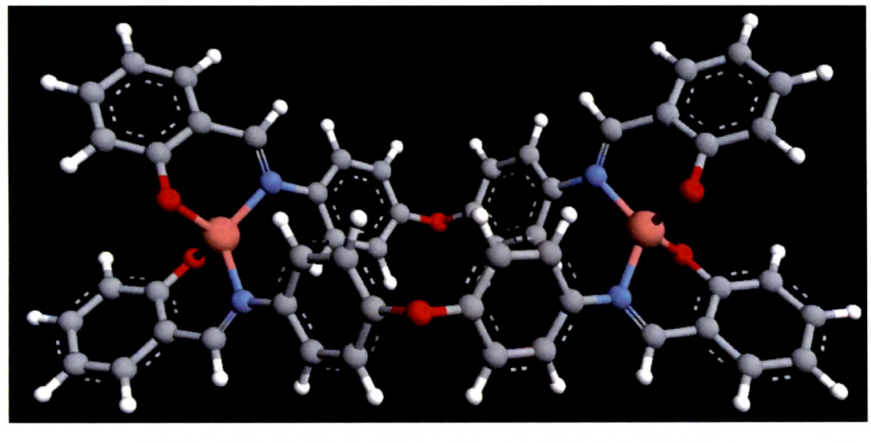

Fig 2.18.3 Optimised geometry of $[Cu_2(salDPE)_2]$

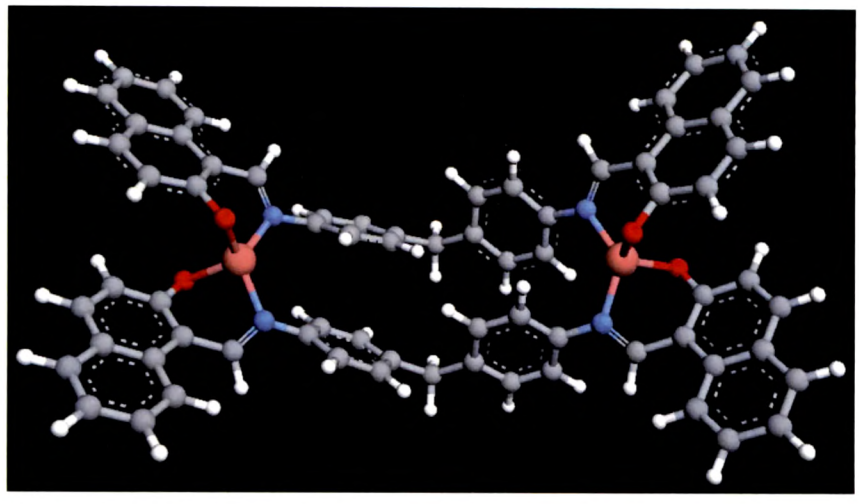

Fig 2.18.4 Optimised geometry of $[Cu_2(naphDPM)_2]$

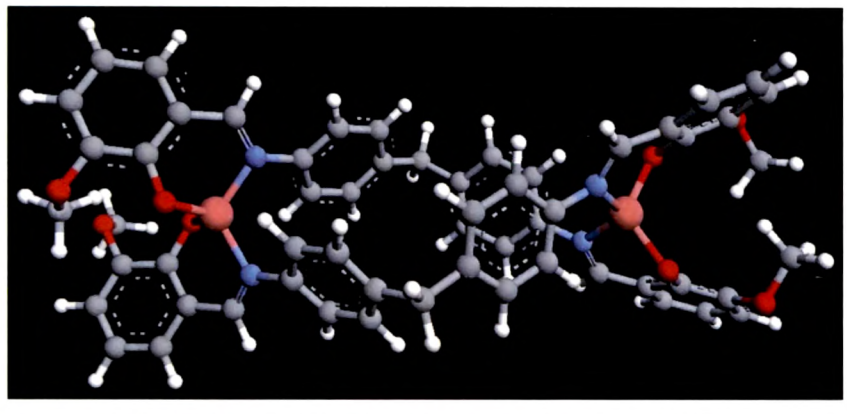

Fig 2.18.5 Optimised geometry of $[Cu_2(vanDPM)_2]$

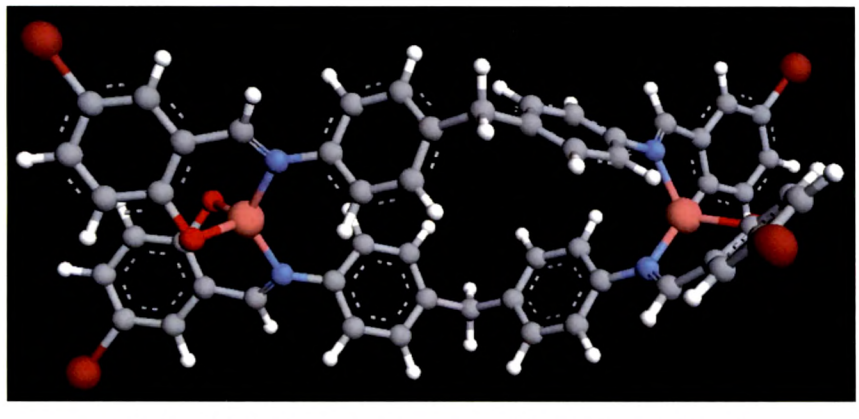

Fig 2.18.6 Optimised geometry of $[Cu_2(BrsalDPM)_2]$

Table 2.7: J, torsional angle and g of some complexes.

Complexes	J (cm^{-1})	Torsional angle	g
$[Cu_2(salDPM)_2].(H_2O)_4$	-7.24	175.3	2.14
$[Cu_2(sal4\text{-}DPS)_2].(H_2O)_2$	12.98	172.55	2.02
$[Cu_2(salDPE)_2].H_2O$	39.02	170.0	1.98
$[Cu_2(naphDPM)_2]$	27.19	172.29	2.02
$[Cu_2(vanDPM)_2].H_2O$	27.07	136.48	1.93
$[Cu_2(BrsalDPM)_2]$	53.16	129.08	1.84
$[Cu_2(sal3\text{-}DPS)_2].(H_2O)_3$	47.33	177.79	2.02

The trends in the **Table 2.7,** indicate that the extent of spin exchange depends largely on the torsional angle between metal coordination planes. The J values indicate greater ferromagnetic interaction with greater deviation in torsional angle from 180°.

A comparison between the complexes, $[Cu_2(salDPM)_2]$, $[Cu_2(sal4\text{-}DPS)_2]$ and $[Cu_2(salDPE)_2]$, where the ligands differ only in the central functionality holding the bis-phenyl moieties, indicates that the deviation in torsional angle increases from linearity in the order $[Cu_2(salDPM)_2] < [Cu_2(sal4\text{-}DPS)_2] < [Cu_2(salDPE)_2]$. Consequently, the $[Cu_2(salDPM)_2]$ is weakly antiferromagnetic while the others are moderately ferromagnetic with $[Cu_2(salDPE)_2]$ complex having highest J value of the three.

The complexes $[Cu_2(salDPM)_2]$, $[Cu_2(naphDPM)_2]$, $[Cu_2(vanDPM)_2]$ and $[Cu_2(BrsalDPM)_2]$, have same bridging functionality while the non-bridging part has different functional groups. The deviation in torsional angle from 180° increase in the order,

$[Cu_2(salDPM)_2] < [Cu_2(naphDPM)_2] < [Cu_2(vanDPM)_2] < [Cu_2(BrsalDPM)_2]$.

The J values also increase in the order $[Cu_2(salDPM)_2] < [Cu_2(naphDPM)_2] \approx [Cu_2(vanDPM)_2] < [Cu_2(BrsalDPM)_2]$. Thus there is a significant dependence of J on the torsional angle in these complexes.

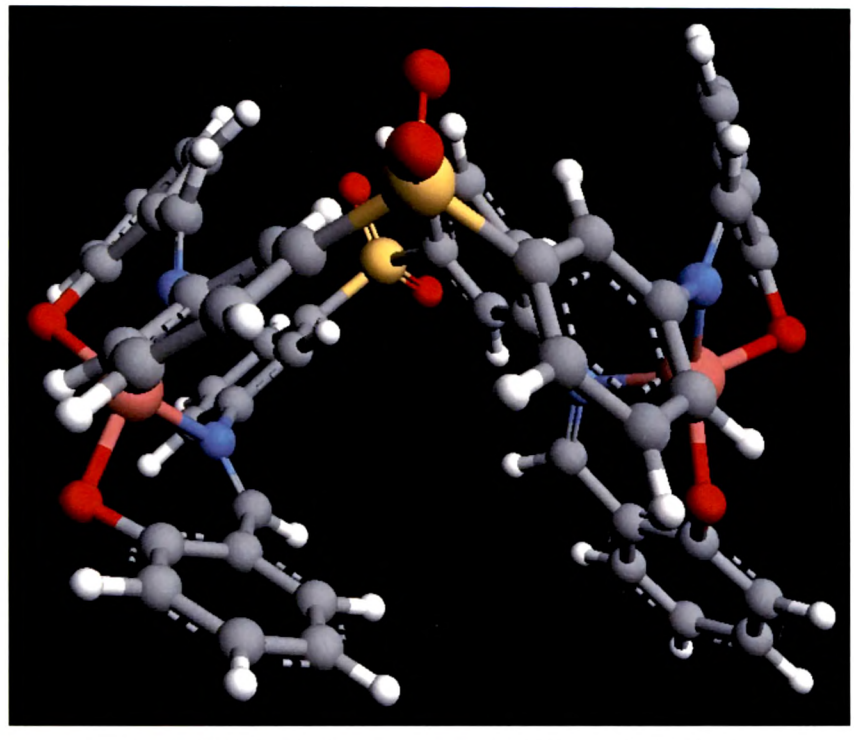

Fig 2.18.7 Optimised geometry of $[Cu_2(sal3\text{-}DPS)_2]$

$[Cu_2(sal3DPS)_2]$ appears to be an exception because the deviation in torsional angle between metal coordination planes is less i.e. 177.79 but J is higher. In this molecule $-SO_2-$ group occupies meta position to the coordinating site and this has two effects (i) the delocalization of metal electron/spin density at position 3 that is vital for propagating exchange is less and (ii) the molecule is highly distorted, thus the ligand orbitals with suitable energy have nodes. This hindered effective overlapping between paramagnetic orbitals of copper (II) ions and the molecular orbitals possessed by the bridging ligands. Hence, the metal paramagnetic orbitals are forced to remain degenerate and these results in greater ferromagnetism.

The substitutions over the ligands have a significant effect on the electron density on the two paramagnetic metal centres and hence on the extent of the super exchange interaction. An electron withdrawing group on the ligand reduces the electron density on the metal ion, whereas, an electron releasing group increases the

electron density, with consequent increase and decrease, respectively, of the spin exchange interaction between two metal centres.

The substitution on the ligand may also affect the planarity of the molecule and hence the overlap of the metal orbitals with the orbitals of the bridging atoms.

Thus it can be concluded that the variation in functional groups on the non bridging part of the ligand as well as a minor variation in the bridging group can affect the molecular geometry and hence can have significant effect on the extent of spin exchange between paramagnetic centres through long multiatomic bridges.

2.4 References:

[1] D. Willett, O. Kahn *(Eds), Magneto-Structural Correlations in Exchanged Coupled systems, NATO ASI Series C 140, Reidel Dordrecht, 1985.*

[2] D. Gatteschi, O. Kahn, J. S. Miller, E. Palacio *(Eds). Molecular Magnetic Materials, NATO ASI Series Kluwer, Dordrecht 1991.*

[3] O. Kahn, *Molecular Magnetism, VCH New York 1991.*

[4] Molecular Magnetism : From Molecular Assemblies to the Deviced, E. Coronado, P. Delhaes, D. Gatteschi, J. S. Kluwer, *The Netherlands 1996.*

[5] O. Kahn, *Adv. Inorg. Chem., 1996, 43,179.*

[6] E. S. Solomon, *in copper proteins, (Ed) T. G. Spiro, Wiley-Interscience, New York 1981.*

[7] Copper Coordination Chemistry : Biological and Inorganic perspectives, K. D. Karlin, Zubieta *(Ed), Adenine Press: Guiderland New York, 1983.*

[8] H. C. Liang, M. Dahan, K. D. Karlin, *Curr. Opin. Chem. Biol., 1999, 3 (2), 168.*

[9] S. Schindler, *Eur. J. Inorg. Chem., 2000, 2311.*

[10] H. Borzel, P. Comba, K. S. Hagen, *Inorg. Chem., 2002, **41,** 5440.*

[11] Abdou Saad El-Tabl, *J. Chem. Research (S), 2002, 529.*

[12] W. E. Hatfield, *Comments Inorg. Chem., 1981, **1**, 105.*

[13] T. R. Felthouse, D. N. Hendrickson, *Inorg. Chem.,1978, **9**, 2636.*

[14] V. H. Crawford, H. W. Richardson, J. R. Wasson, D. J. Hodgson, W. E. Hatfield, *Inorg. Chem. 1976, **15**, 2107.*

[15] D. Ajo, A. Bencini, F. Mani, *Inorg. Chem., 1988, 27, 2437.*

[16] T. Ishida, T. Kawakami, Mitsubori, T. Nogami, K. Yamaguchi, H. J. Iwamura, *Chem. Soc. Dalton Trans, 2002, 3177.*

[17] M. Julve, Verdaguer, A. Gleizes, *Inorg. Chem., 1983, 22, 368.*

[18] T. N.Doman, D. E. Williams, J. F. Bankes, R. M. Bunchanan, D. N. Hendrickson, *Inorg. Chem., 1990, **29**, 1058.*

[19] M. Corbett, B. F. Hoskins, *J. C. S. Chem. Commun., 1968, 1602.*

[20] N. D. Kulkarni, P. K. Bhattacharya, *Trans. Met. Chem., 1989, **14**, 303.*

[21] K. Auwers, O. Burger, *Ber. 1904, 37, 3934.*

[22] B. Bleany, K. D. Bowers, *Proc. Roy. Soc. (London), 1952, **A 214**, 451.*

[23] B. Bleany, K. D. Bowers, *Phil. Mag., 1952, **43**, 372.*

[24] V. Mckee, J. Smith, *J. Chem. Commun., 1983, 1645.*

[25] J. A. Barmes, D. J. Hodgson, W. E. Hatfield, *Inorg. Chem., 1972, **11**, 144.*

[26] P. J. Hay, J. C. Thibeault, R. J. Hoffmann, *Am. Chem. Soc., 1975, **97**, 4884.*

[27] A. Bencini, D. Gatteschi, *Inorg. Chim. Acta., 1978, **31**, 11.*

[28] L. Banci, A. Bencini, D. Gatteschi, *J. Am. Chem. Soc., 1983, **105**, 761.*

[29] M. F. Charlot, O. Kahn, S. Jeannin, Y. Jeannin, *Inorg. Chem., 1980, **19**, 1410.*

[30] E. Ruiz, P. Alemany, S. Alvarez, J. Cano, *Inorg. Chem., 1997, **36**, 3683.*

[31] E. Ruiz, P. Alemany, S. Alvarez, J. Cano, *J. Am. Soc., 1997, **119**, 1297.*

[32] B. Graham, M. T. W. Heam, P. C. Junk, C. M. Kepert, F. E. Mabbs, B. Moubaraki, K. S. Murray, L. Spiccia, *Inorg. Chem., 2001, **40**, 1536.*

[33] O. Kahn, *Molecular Magnetism, VCH New York 1993.*

[34] O. Kahn, *Angew. Chem. Int. (Ed.) Engl., 1985, **24**, 834.*

[35] Journal Citations for this Calculation:-

[35.a] M. A. Thompson, M. C. Zerner, *J. Am. Soc., 1991, **113**, 8210.*

[35.b] M. A. Thompson, E. D. Glendening, D. Feller, *J. Phys. Chem., 1994, **98**, 10465.*

[35.c] M. A. Thompson, G. K. Schenter, *J. Phys. Chem., 1995, **99**, 6374.*

[35.d] M. A. Thompson, *J. Phys. Chem., 1996, **100**, 14492.*

[36] UFF references:-

[36.a] A. K. Rappe, et. al., *JACS, 1992, **114**, 10024.*

[36.b] C. J. Casewit, K. S. Colwell, A. K. Rappe, *JACS, 1992, **114**, 10035.*

[36.c] C. J. Casewit, K. S. Colwell, A. K. Rappe, *JACS, 1992, **114**, 10046.*

[36.d] A. K. Rappe, W. A. Goddard, *JPC, 1991, **95**, 3358.*

[36.e] A. K. Rappe, K. S. Colwell, C. J. Casewit, *Inorg. Chem., 1993, **32**, 3438.*